Geomechanics and Engineering, *Vol. 15, No. 3 (2018) 823-831*
DOI: https://doi.org/10.12989/gae.2018.15.3.823

Critical face pressure and backfill pressure in shield TBM tunneling on soft ground

Kiseok Kim[1b], Juyoung Oh[2a], Hyobum Lee[3b], Dongku Kim[3b] and Hangseok Choi[*3]

[1]*Department of Civil and Environmental Engineering, University of Illinois, IL, U.S.A.*
[2]*Samsung C&T Corporation, Seoul, Korea*
[3]*School of Civil, Environmental and Architectural Civil Engineering, Korea University, Seoul, Korea*

(Received May 8, 2017, Revised February 12, 2018, Accepted March 23, 2018)

Abstract. The most important issue during shield TBM tunneling in soft ground formations is to appropriately control ground surface settlement. Among various operational conditions in shield TBM tunneling, the face pressure and backfill pressure should be the most important and immediate measure to restrain surface settlement during excavation. In this paper, a 3-D hydro-mechanical coupled FE model is developed to numerically simulate the entire process of shield TBM tunneling, which is verified by comparing with real field measurements of ground surface settlement. The effect of permeability and stiffness of ground formations on tunneling-induced surface settlement was discussed in the parametric study. An increase in the face pressure and backfill pressure does not always lead to a decrease in surface settlement, but there are the critical face pressure and backfill pressure. In addition, considering the relatively low permeability of ground formations, the surface settlement consists of two parts, i.e., immediate settlement and consolidation settlement, which shows a distinct settlement behavior to each other.

Keywords: TBM; face pressure; backfill pressure; consolidation; tunneling

1. Introduction

The construction of tunnels has considerably increased during the last few decades in urban areas because of the growing demand for development of underground space to accommodate underground facilities such as subways, underground roads, water and sewage tunnels and gas tunnels. In constructing a new tunnel, the proximity of these underground facilities from one to another becomes unavoidable, and underground space is getting more complicated (Ding *et al.* 2017, Hyun *et al.* 2015, Zheng *et al.* 2017).

In general, conventional tunneling methods have been employed in urban areas. But, for soft ground formations under the ground water level, the conventional methods cannot appropriately cope with the ground subsidence (Ward and Pender 1981). As the excavation technology has improved, the subsidence can now be controlled by shield tunneling, using shield Tunnel Boring Machines (TBMs) that adopts a rigid steel protector to support the ground and apply pressure on the tunnel face and tail void, and then fulfills excavation safely.

Even with the current rise of computer technology and high-performance numerical methods, a clear standard of numerical analysis for a shield tunneling process does not exist because the numerical analysis for simulating shield TBM tunneling is extremely complicated and requires a number of inevitable assumptions (Kasper 2004, Jun and Kim 2015, Lee 2012, Nawel and Salah 2015, Swoboda and Abu-Krisha 1999).

In this paper, a 3-D hydro-mechanical coupled FE model is developed to numerically simulate the entire process of shield TBM tunneling construction in less permeable ground, in which consolidation may occur. The FE analysis simulating the excavation of a slurry shield TBM was facilitated along with the commercial program ABAQUS (v. 6.14), which was verified by comparing with the field data obtained from the Hong-Kong site (Park *et al.* 2016). In the parametric study, the effect of permeability and stiffness of ground formations on tunneling-induced surface settlement during shield TBM tunneling was discussed. The main purpose of this paper is to study the influence of operational conditions on the ground surface settlement. Among various operational conditions in shield TBM tunneling, the face pressure and backfill pressure are considered to be the most important and immediate factor to restrain surface settlement during excavation (Oh and Ziegler 2013). In dealing with a relatively less permeable ground formations, the surface settlement consists of two parts, i.e., immediate settlement and consolidation settlement, which shows a distinct settlement behavior to each other (Ata 1996). From a construction management perspective during shield TBM tunneling, the immediate settlement attracts a shot-term effect of tunnel construction on the ground surface deformation (Lewis and Schrefler 2000). On the other hand, the consolidation settlement is related to a long-term management issue after completion of tunnel construction (Au *et al.* 2003). The influence of face pressure and backfill pressure on the surface settlement was

∗Corresponding author, Professor
E-mail: hchoi2@korea.ac.kr
[a]Ph.D.
[b]Ph.D. Student

ISSN: 2005-307X (Print), 2092-6219 (Online)

discussed by introducing a new concept of critical pressure.

2. FE modeling for shield TBM tunneling

2.1 Numerical modelling

The FE model for slurry shield TBM tunneling consists of 4 parts: ground formation, grout, shield and lining (Fig. 1). The solid element modeled for the ground formation and the grout is composed of 20-nodes to make a quadratic displacement approximation. To simulate the two-phase formulation (ground (solid) and water), an additional degree of freedom is assigned to 8 corner nodes to represent pore water pressure, and the values between the nodes are approximated by linear interpolation. The grout was regarded as a saturated porous material. The reduction in permeability of hydrating cement at the early stage was considered. The hydration process was assumed to be time-dependent, and the exponential function proposed by Kasper (2004) was applied to describe the decrease in permeability of grout (Fig. 2). The shield was designed in a cylindrical shape with conicity modeled with shell elements. By assigning much higher stiffness in relation to the ground, the shield machine was regarded as a rigid body. For simplicity, the segment lining was modeled as a continuous, elastic tube using square volume elements only with the displacement approximation. The designated elements were activated at each step of the segment installation.

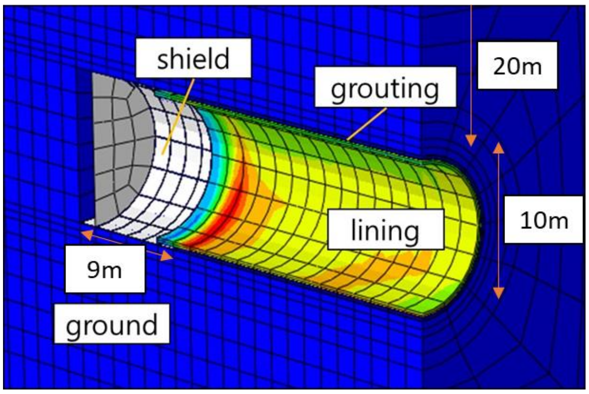

Fig. 1 Parts of the FE model for shield TBM excavation

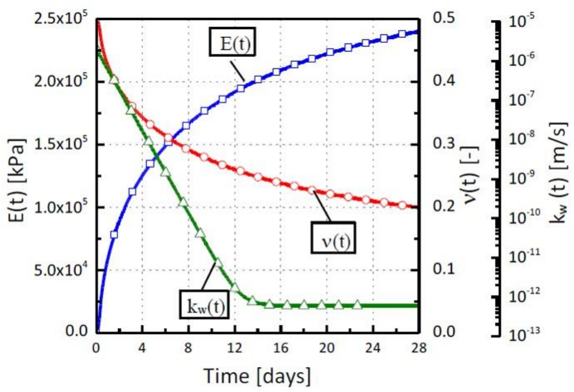

Fig. 2 Time-dependent stiffness and permeability of grout

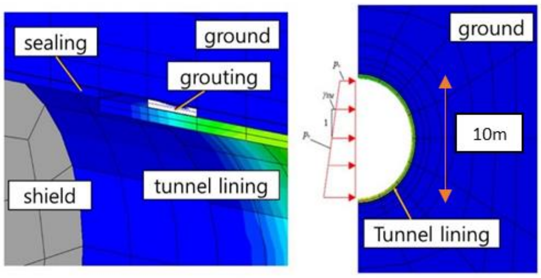

Fig. 3 Modeling of grouting pressure

In order to implement the boundary conditions in the numerical model for slurry shield TBM tunneling, only one half of the tunnel was considered, and the horizontal displacements were restricted on the symmetry plane. The vertical displacements at the front, rear, and side planes were set to be zero. The ground water level was assumed to be on the ground surface, and the boundary condition of pore water pressure was formulated as hydrostatic on the lateral level (Anagnostou 1995). These boundary conditions remained undisturbed during the numerical simulation. The outer boundaries including the symmetry plane were assumed to be impermeable.

In the course of excavation of a shield TBM, the stability of face is extremely important to ensure stable ground formations. The shield machine excavates the ground in the face, which is pressurized (i.e., face pressure) by slurry (in the slurry shield TBM) or excavated earthen materials (in the EPB shield TBM). Especially in the slurry shield TBM, it is assumed that the filter cake is formed completely on the surface of tunnel face, and the slurry-induced linear pressure distribution over the height of the face is exerted. Assuming that ground deformation at the tunnel face is small, the face pressure at the crown is adjusted according to the total primary stress. The backfill pressure applied into the annular gap by grouting causes an additional load transferred to the ground and the segment lining. The magnitude and implementation of backfill pressure in the model is illustrated in Fig. 3. The unit weight of the pressurized mortar, was assumed to be $21\ kN/m^3$ in the current numerical model.

The driving of a shield TBM was simulated by adopting the activation and deactivation application. After a certain excavation stage, the existing elements of the shield machine and the existing contact should be deactivated, and at the same time, the new elements of the shield machine and the corresponding contacts, which are 1.5 m (advance length) ahead, were activated. After the shield advances along with lining installation, the backfill pressure was applied on the excavation surface and the segment lining. Subsequently, the first elements of grout were activated at the same time, and these elements were loaded, and the existing pressure was released. After this step, the new tunnel lining and contacts were activated. These simulation steps were repeated until the shield machine completed excavation. After the excavation, an additional calculation step took place to simulate the consolidation process.

2.2 Constitutive model for ground

Considering a stress-stain relation of the ground

Table 1 Parameters for hypoplastic model

γ_{sat}	$21kN/m^3$	e_{i0}	1.05
φ_c	33°	α	0.25
h_s	$1.5\times10^6 kPa$	β	1.5
n	0.28	m_R	5.0
e_{d0}	0.55	m_T	2.0
e_{c0}	0.95	χ	6.0

*γ_{sat}: saturated unit weight, φ_c: critical friction angle, h_s: granular stiffness, n: compression exponent, e_{d0}: void ratio at maximum compaction in a stress-free state, e_{c0}: critical void ratio in a stress-free state, e_{i0}: void ratio at minimum compaction in a stress-free state, α: pycnotropy exponent, β: barotropy exponent, m_R: increase factor at a 180° change in direction, m_T: increase factor at a 90° change in direction, χ: maximum intergranular exponent

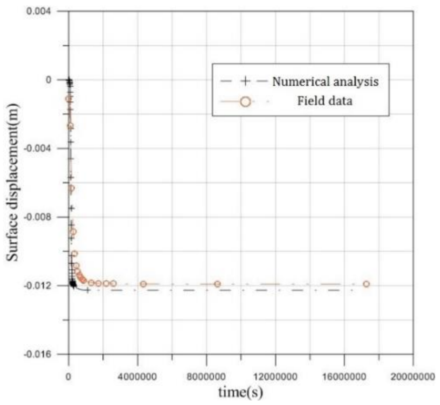

Fig. 4 Comparison of numerical analysis with field measurement

formation, the hypoplastic model was adopted as a constitutive model that was proposed by von Wolffersdorff (1996), in which the non-linear stress-strain relation, and the dependency of the stress level and relative density can be considered. The hypoplastic model expresses the stress-strain relationship in terms of time rate variables to define the inelastic behavior by the modulus of strain rate. In addition, the stiffness of ground formation was assumed to be proportional to the stress level as shown in Eq. (1) (Herle and Gudehus 1999, Herle and Kolymbas 2004).

$$\dot{\sigma} = C_1\sigma\dot{\varepsilon} + C_2\sigma|\dot{\varepsilon}| \quad (1)$$

Because the von Wolffersdorff model is able to consider a change in void ratio during loading/unloading, a unique relationship can be adopted for both loading and unloading without any intentional classification between elastic and plastic deformations. In a tensor notation, the stress rate tensor ($\dot{T}_s$) is determined in function of the strain rate (D), skeleton (effective) stress (T_s), and void ratio (e) (refer to Eq. (2)) (Bauer 1996).

$$\dot{T}_s = h(T_s, D, e) \quad (2)$$

In formulating the hypoplastic model, various parameters should be input into the model. In Table 1, the parameters for the hypoplastic model in this study are presented and explained.

2.3 Model verification

The field measurements obtained from a Hong Kong slurry-type shield tunneling site were examined. The numerical analysis modeled for the given conditions was compared with the field measurements as shown in Fig. 4. For comparison with the field data, the slurry-type shield TBM numerical analysis model was used in this paper. It is shown that the surface settlement simulated by the numerical model was fairly similar to the field data.

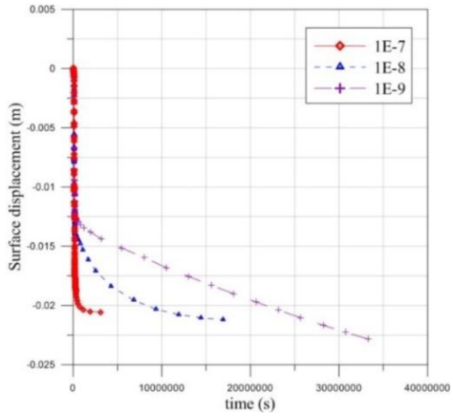

Fig. 5 Ground surface settlement corresponding to hydraulic conductivity

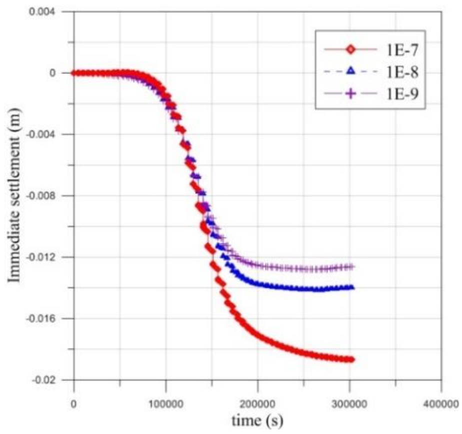

(a) Immediate settlement

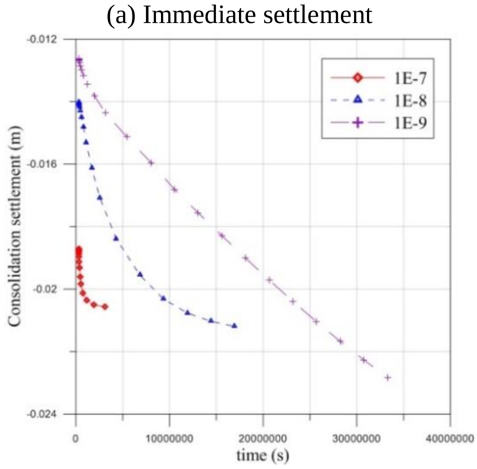

(b) Consolidation settlement

Fig. 6 Effect of ground permeability on immediate and consolidation settlement

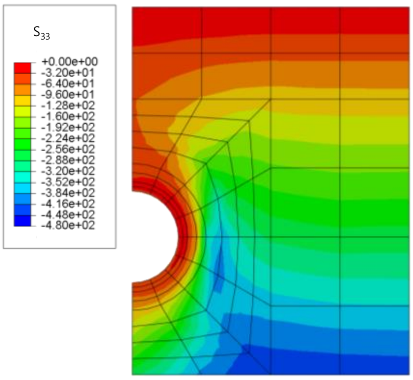

(a) $\mathrm{k} = 1 \times 10^{-7} m/s$

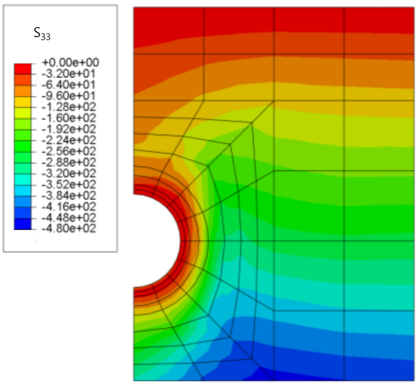

(b) $\mathrm{k} = 1 \times 10^{-8} m/s$

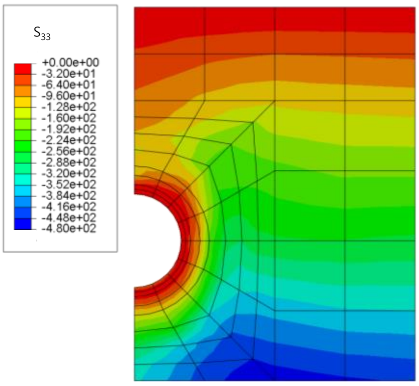

(c) $\mathrm{k} = 1 \times 10^{-9} m/s$

Fig. 7 Vertical effective stress distribution after application of backfill pressure

3. Parametric study for ground conditions

3.1 Permeability of ground

The influence of permeability of ground formations on the immediate and consolidation settlement was discussed in this section. A typical hydraulic conductivity of ground was assumed to be $1 \times 10^{-8} m/s$ in order to exert consolidation during shield TBM tunneling. In addition, two comparative values of $1 \times 10^{-7} m/s$ and $1 \times 10^{-9} m/s$ were chosen. The consolidation analysis was conducted for the period of 2 years until convergence. The ground surface settlement with time corresponding to each hydraulic conductivity is presented in Fig. 5. In addition, the immediate settlement and consolidation settlement are separately illustrated in Fig. 6. The consolidation settlement indicates the additional ground deformation after the immediate settlement for each hydraulic conductivity.

The results show that an increase in permeability increases the immediate settlement, but reduces the consolidation settlement because the application of face pressure and backfill pressure exerts more effective stress with less excess porewater pressure at the vicinity of the tunnel in more permeable ground formations. In other words, as the permeability of ground formations gets smaller, the less effective stress is generated near the tunnel, which causes less immediate settlement, but more consolidation settlement should be expected due to the occurrence of more excess porewater pressure. As the permeability of ground formations decreases, there is not enough time to induce a change in effective stress responding to the application of face pressure and backfill pressure. This aspect of change in effective stress according to the permeability of ground is illustrated in Fig. 7, which indicates the effective stress distribution in the vertical direction right after the application of backfill pressure. In addition, as the hydraulic conductivity becomes higher, the reduction of the vertical stresses above the tunnel crown, and the increase in vertical stresses at around 0.5D away from the tunnel side wall get more significant.

3.2 Stiffness of ground

The influence of stiffness of ground formations on the immediate and consolidation settlement was discussed in this section. Four different Young's moduli were chosen to represent a typical less permeable ground condition (such as a clay deposit), i.e., 14.8, 24.8, 32.5 and 50.2 MPa. The selected Young's moduli are back calculated to correspond to the ground stiffness controlled by the granular stiffness (h_s) in the hypoplastic model.

The total settlement including the immediate and consolidation settlement of ground surface is illustrated in Fig. 8. It is reasonable that a decrease in the stiffness of ground formations induces an increase in both immediate and consolidation settlement. In addition, the magnitude of excess porewater pressure induced by the application of face pressure and backfill pressure is higher in case of the lower stiffness as shown in Fig. 9, which also requires more time to dissipate the excess porewater pressure.

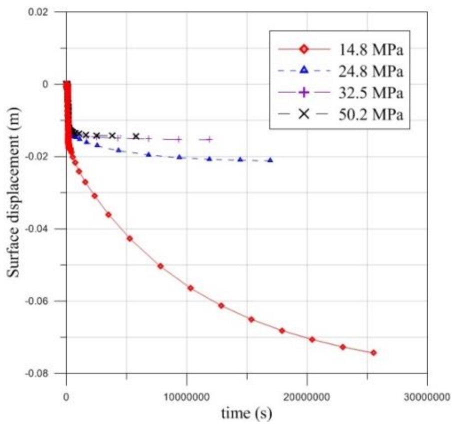

Fig. 8 Effect of ground stiffness on surface settlement

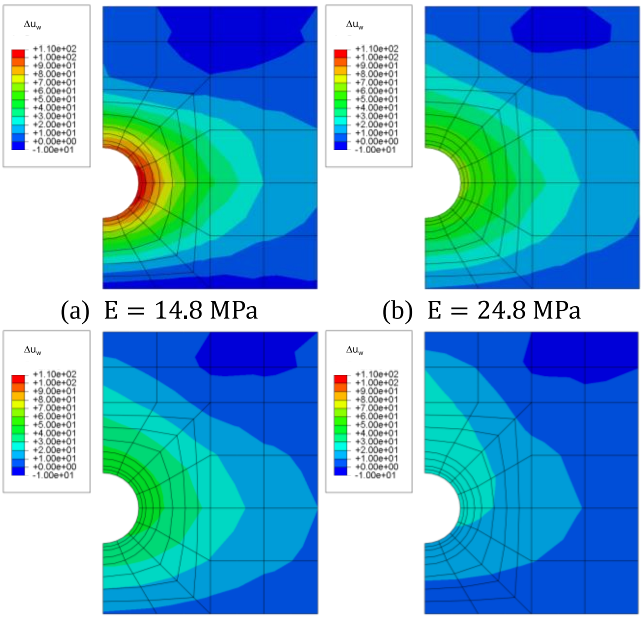

(a) E = 14.8 MPa (b) E = 24.8 MPa

(c) E = 32.5 MPa (d) E = 50.2 MPa

Fig. 9 Excess porewater pressure distribution before consolidation

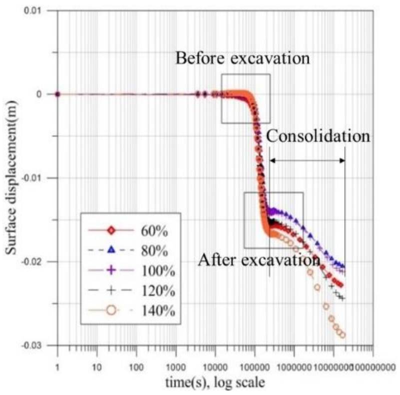

Fig. 10 Surface settlement corresponding to face pressure

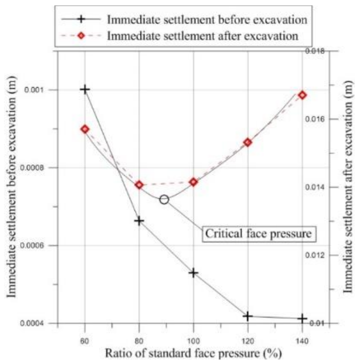

Fig. 11 Immediate settlements before & after excavation

4. Influence of operational conditions on surface settlement

The magnitude of face pressure is significantly important to accomplish a successful slurry shield TBM excavation along with a high level of deformation control. Five different values of face pressure (i.e., 60%, 80%, 100%, 120% and 140% of the typical face pressure) were adopted to study the effect of face pressure on the immediate and consolidation settlements. The typical face pressure was defined as the initial stress in ground including the pore pressure before excavation. The surface settlements are expressed in the logarithmic time scale in Fig. 10. As mentioned previously, the surface settlement is divided into the immediate and consolidation settlement. The immediate settlement can be defined in two steps, that is, before excavation and after excavation. The two steps of immediate settlements are boxed in Fig. 10. The immediate settlements in the box in Fig. 10 are re-plotted corresponding to the face pressure in Fig. 11 to observe the critical face pressure. The immediate settlement before excavation and after excavation is compared to each other in Fig. 11. As the face pressure increases from 60% to 140% of the typical face pressure, it is noted that the immediate settlement before excavation is reduced. The immediate settlement after excavation shows a different tendency. As the face pressure increases from 60% to 80% of the typical face pressure, the immediate settlement gradually decreases to the minimum value. Beyond this minimum value, the immediate settlement begins to increase with an increase in the face pressure. Therefore, assessment of the immediate settlement after excavation suggests a concept of critical face pressure, which indicates the face pressure leading to the minimum immediate settlement.

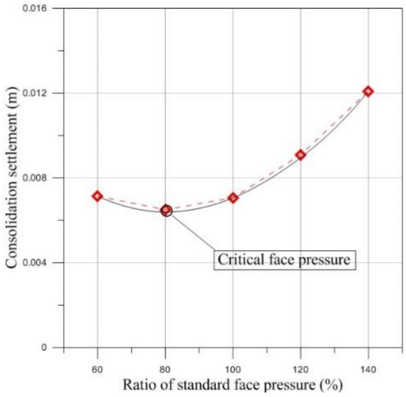

Fig. 12 Consolidation settlement corresponding to face pressure

For the consolidation stage, the consolidation settlement with respect to the magnitude of face pressure is presented in Fig. 12. The concept of critical face pressure exists in the consolidation settlements as well, which results in the minimum consolidation settlement. That is, the consolidation settlement increases along with the application of face pressure beyond this critical value. In practice, the application of excessively large face pressure may cause a risky long-term condition due to substantial consolidation settlement.

The effect of face pressure can be evaluated in three main steps: 1) Before excavation, 2) After excavation, 3) After consolidation. The tendency of immediate settlement is discussed along with the vertical effective stress distribution around the tunnel at each excavation stage.

The surface settlement occurs due to a change in the stress field. In Fig. 13, the stress distribution in the ground formation is delineated when the face pressure is applied. When the face pressure increases from 60% to 80% of the typical face pressure, the stress field around the tunnel does not change significantly from the initial state. But, from 80% to 140%, the stress change increases.

After excavation, the stress relaxation occurs in the vicinity of the tunnel. The stress distribution after excavation is almost similar, because all the stress on the excavation surface has been relaxed. As a result, in Fig. 11 when the face pressure increases from 60% to 80% of the typical face pressure, the magnitude of settlement decreases, whereas from 80% to 140%, the magnitude of settlement increases. Therefore, the critical face pressure exists in the immediate settlement as mentioned previously.

The existence of critical face pressure in the immediate settlement can be phenomenologically explained. When the excavation begins, the face pressure is applied on the face, and affect the stress state in front of the face. Before the face pressure becomes too large, the face pressure makes an increase in the confined stress. But, as the face pressure exceeds a certain pressure, the increase in the face pressure acts as an increase in deviatoric stress.

For the consolidation settlement, the total and effective stress are compared for a certain face pressure as shown in Fig. 14. It can be seen that the total stress converges earlier compared to the effective stress. It means that consolidation occurs as the effective stress changes. By comparing the effective stress change corresponding to the face pressure, the critical face pressure is confirmed as shown in Fig. 15.

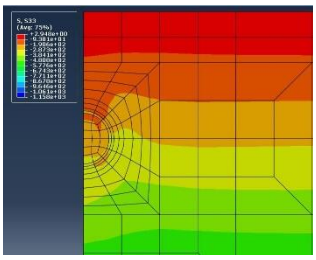
(a) 60%

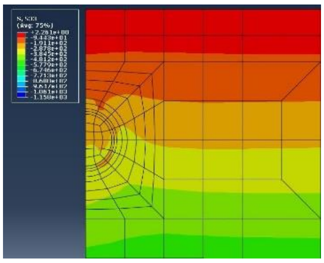
(b) 80%

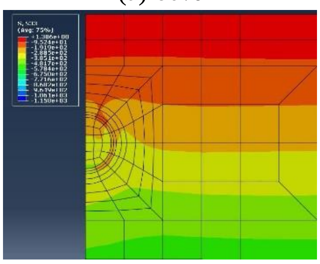
(c) 100%

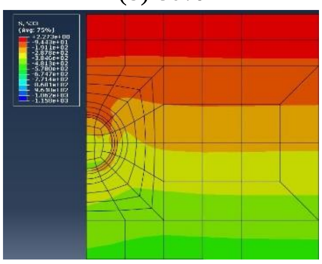
(d) 120%

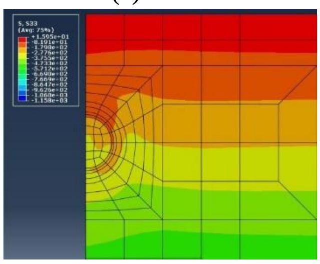
(e) 140%

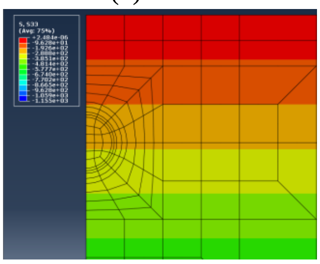
(f) Initial state

Fig. 13 Vertical effective stress distribution in ground right before excavation

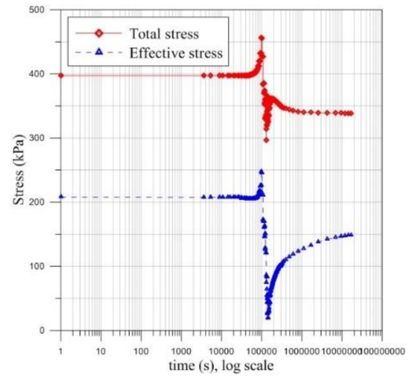

Fig. 14 Effective stress and total stress during excavation and consolidation

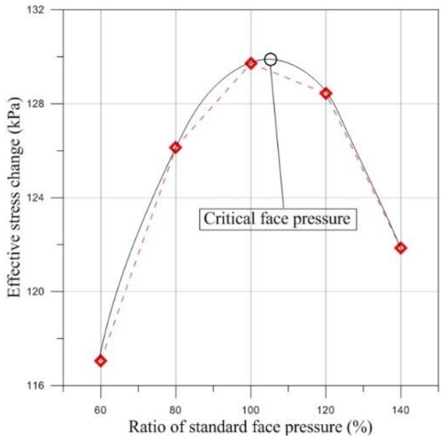

Fig. 15 Effective stress change at consolidation settlement with respect to face pressure

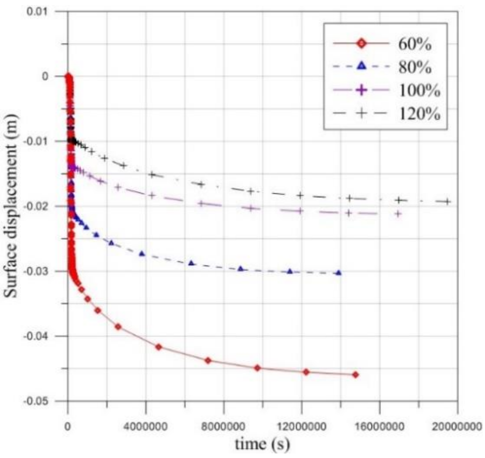

Fig. 16 Surface settlement according to backfill pressure

4.2 Backfill pressure

Four cases of backfill pressure were considered to study the effect of backfill pressure. The typical backfill pressure was selected as the pressure at each elevation, which is linearly distributed from the crown to reflect the grout weight. Backfill pressures of 60%, 80%, 100% and 120% of the typical backfill pressures were considered.

In Fig. 16, the surface settlements corresponding to each backfill pressure are illustrated. As the backfill pressure

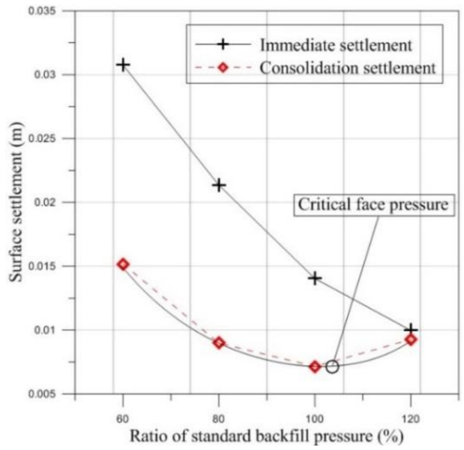

Fig. 17 Immediate settlement and consolidation settlement according to backfill pressure

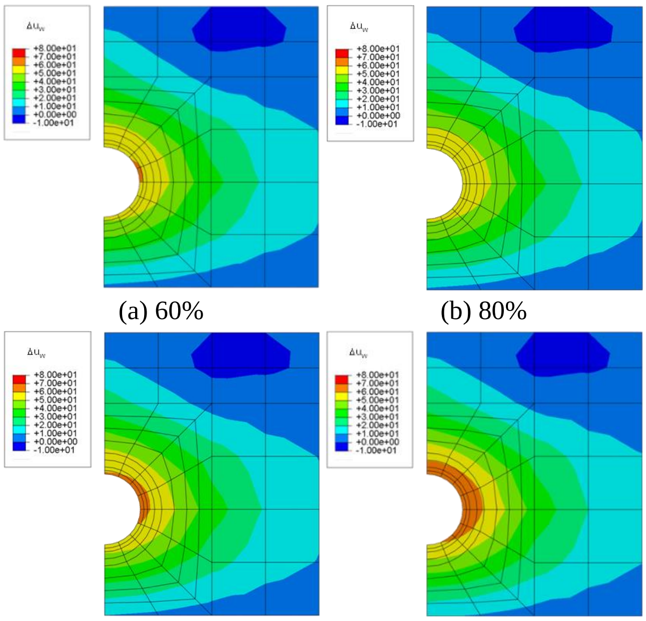

(a) 60% (b) 80%

(c) 100% (d) 120%

Fig. 18 Excess porewater pressure after excavation (before consolidation)

increases, it is clearly confirmed that the immediate settlement gradually decreases with no minimum value (refer to Fig. 17). However, the consolidation settlement shows a different tendency. At the backfill pressure near 100% of the typical backfill pressure, the consolidation settlement becomes the minimum. Beyond this minimum value, the consolidation settlement begins to increase with an increase in the backfill pressure. This shows the existence of the critical backfill pressure.

The distribution of excess porewater pressure is described in Fig. 18. The excess porewater pressure around the tunnel increases as the backfill pressure increases. Unfortunately, the distribution of excess porewater pressure cannot identify the existence of critical backfill pressure. In the pursuit of this purpose, it is necessary to compare the distribution of vertical effective stress around the tunnel before and after consolidation as shown in Fig. 19 and 20.

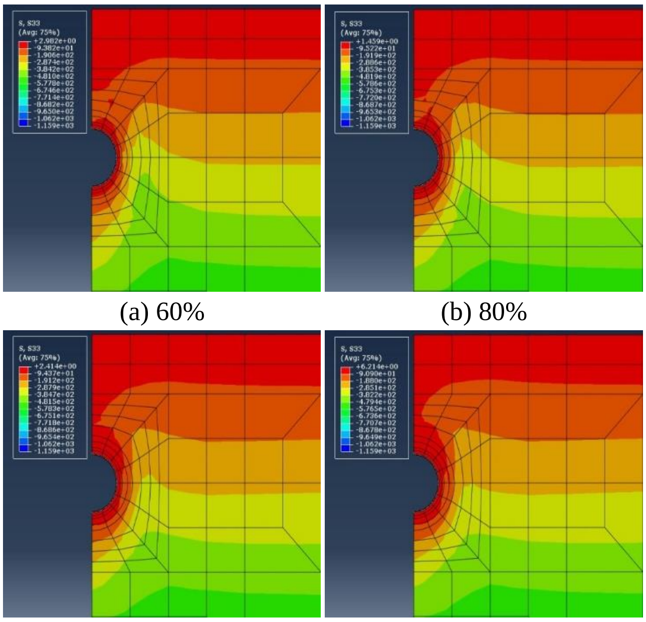

(a) 60% (b) 80%

(c) 100% (d) 120%

Fig. 19 Distribution of vertical effective stress after excavation (before consolidation)

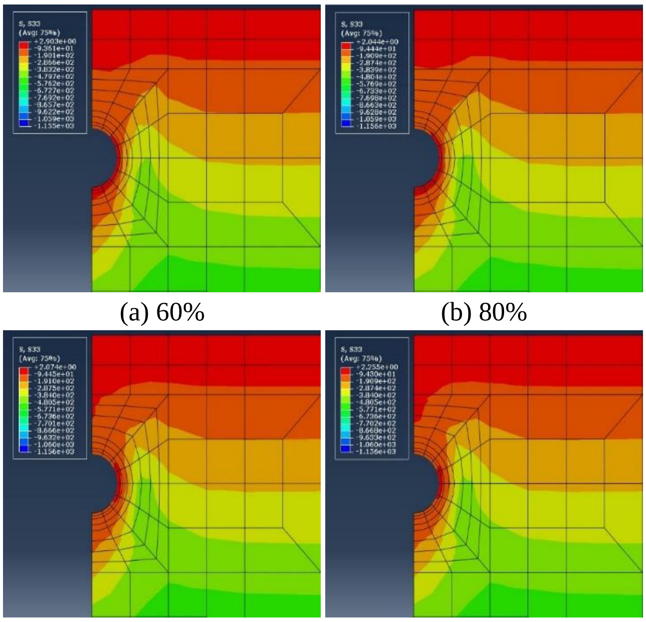

(a) 60% (b) 80%

(c) 100% (d) 120%

Fig. 20 Distribution of vertical effective stress after consolidation

As the backfill pressure increases, the effective stress around the tunnel before consolidation increases. However, in the course of consolidation, the maximum increment of vertical effective stress is not observed in case of the largest backfill pressure. This indicates that the critical backfill pressure exists in the range of backfill pressure (i.e., between 60% and 120% of the typical backfill pressure).

The vertical effective stress change (from before-consolidation to after-consolidation) decreases when the backfill pressure increase from 60% to 80% of the typical backfill pressure, but increases again to 120%. This means

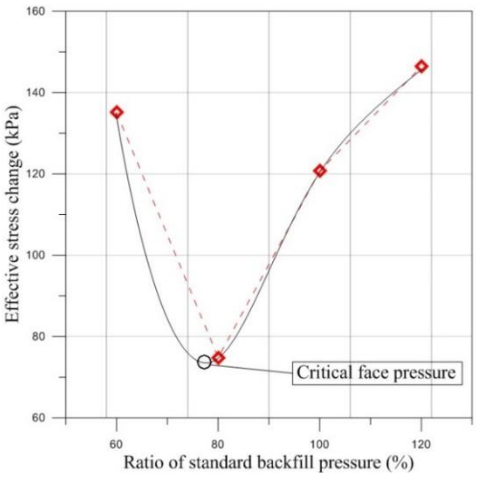

Fig. 21 Vertical effective stress change corresponding to backfill pressure

that the consolidation settlement will also decrease as an increase in the backfill pressure from 60% to 80% of the typical backfill pressure, and increase again to 120%, which indicates the critical backfill pressure (refer to Fig. 21).

5. Conclusions

In this paper, comprehensive numerical studies on shield TBM tunneling were carried out, and the key findings are summarized as follows:

• A 3D hydro-mechanical coupled FE numerical model was developed to simulate the entire process of shield TBM tunneling. The numerical model was verified by comparing with the real field data obtained from an actual slurry shield TBM tunneling in Hong Kong.

• An increase in the permeability of ground formations increases the immediate settlement, but reduces the consolidation settlement because the application of face pressure and backfill pressure exerts more effective stress and less excess porewater pressure at the vicinity of the tunnel. A decrease in the stiffness of ground formations induces an increase in both immediate and consolidation settlement. However, the rate of consolidation settlement decreases when the stiffness decreases because of larger magnitude of excess porewater pressure exerted by the application of face pressure and backfill pressure, which requires more time to dissipate the excess porewater pressure.

• With consideration of the effect of face pressure, a concept critical face pressure is introduced, which exists in both the immediate settlement and consolidation settlement. This means that an increase in face pressure does not always guarantee a decrease in ground settlement.

• For the backfill pressure, as the backfill pressure increases, the immediate settlement gradually decreases with no minimum value. However, for the consolidation settlement, the critical backfill pressure exists. That is, an increase in the backfill pressure does not always lead to a decrease in the consolidation settlement.

• Due to the existence of the critical pressures, the application of operational pressures (i.e., face pressure and backfill pressure) excessively greater than the critical pressure can make the ground condition unstable.

Acknowledgements

The authors appreciate the support partially by the Korea Agency for Infrastructure Technology Advancement under the Ministry of Land, Infrastructure and Transport of the Korean government (No. 13SCIP-B066321-01) and (No. 16SCIP-B108153-02).

References

Anagnostou, G. (1995), "The influence of tunnel excavation on the hydraulic head", *J. Numer. Anal. Meth. Geomech.*, **19**(10), 725-746.

Ata, A.A. (1996), "Ground settlements induced by slurry shield tunnelling in stratified soils", *Proceedings of the International Conference on North American Tunnelling '96*, Washington, D.C., U.S.A., April.

Au, S.K.A., Soga, K., Jafari, M.R., Bolton, M.D. and Komiya, K. (2003), "Factors affecting longterm efficiency of compensation grouting in clays", *J. Geotech. Geoenviron. Eng.*, **129**(3), 254-262.

Bauer, E. (1996), "Calibration of a comprehensive hypoplastic model for granular materials", *Soil. Found.*, **36**(1), 13-26.

Ding, Z., Wei, X.J. and Wei, G. (2017), "Prediction methods on tunnel-excavation induced surface settlement around adjacent building", *Geomech. Eng.*, **12**(2), 185-195.

Herle, I. and Gudehus, G. (1999), "Determinatioin of parameters of a hypoplastic constitutive model from properties of grain assemblies", *Mech. Cohes-Frict. Mater.*, **4**(5), 461-486.

Herle, I. and Kolymbas, D. (2004), "Hypoplasticity for soils with low friction angles", *Comput. Geotech.*, **31**(5), 365-373.

Hyun, K.C., Min, S., Choi, H., Park, J. and Lee, I.M. (2015) "Risk analysis using fault-tree analysis (FTA) and analytic hierarchy process (AHP) applicable to shield TBM tunnels", *Tunn. Undergr. Sp. Technol.*, **49**, 121-129

Jun, G.C. and Kim, D.H. (2015), "A interaction on the estimating shield TBM tunnel face pressure through analytical and numerical analysis", *J. Kor. Tunn. Undergr. Sp. Assoc.*, **17**(3), 306-317.

Kasper, T. (2004) "Finite Element Simulation maschineller Tunnelvortriebe in wassergesättigtem Lockergestein", Ph.D. Dissertation, Ruhr University Bochum, Bochum, Germany.

Lee, G.T.K. and Ng, C.W.W. (2002), "Three-dimensional analysis of ground settlements due to tunnelling: role of K0 and stiffness anisotropy" *Proceedings of the International Symposium on Geotechnical Aspects of Underground Construction in Soft Ground*, Toulouse, France, October.

Lewis, R.W. and Schrefler, B.A. (2000), *The Finite Element Method in the Static and Dynamic Deformation and Consolidation of Porous Media*, John Wiley & Sons.

Nawel, B. and Salah, M. (2015), "Numerical modeling of two parallel tunnels interaction using three-dimensional Finite Elements Method", *Geomech. Eng.*, **9**(6), 775-791.

Oh, J.Y. and Ziegler, M. (2013) "Influence of tail void grouting on the surface settlements during shield tunneling", *Proceedings of the International Symposium on Tunneling and Underground Space Construction for Sustainable Development, Korea*, Seoul, Korea, March.

Park, H., Oh, J.Y., Chang, S. and Lee, S. (2016), "Case study of volume loss estimation during slurry TBM tunnelling in weathered zone of granite rock", *J. Kor. Tunn. Undergr. Sp. Assoc.*, **18**(1), 61-74

Swoboda, G. and Abu-Krisha, A. (1999), "Three-dimensional numerical modelling for TBM tunnelling in consolidated clay", *Tunn. Undergr. Sp. Technol.*, **14**(3), 327-333.

von Wolffersdorff, P.A. (1996), "Hypoplastic relation for granular material with a predefined limit state surface", *Mech. Cohes-Frict. Mater.*, **1**(3), 251-271.

Ward, W.H. and Pender, M.J. (1981), "Tunnelling in soft ground-General report", *Proceedings of the 10th International Conference on Soil Mechanics and Foundation Engineering*, Stockholm, Sweden, June.

Zheng, G., Du, Y., Cheng, X., Diao, Y., Deng, X. and Wang, F. (2017), "Characteristics and prediction methods for tunnel deformations induced by excavations", *Geomech. Eng.*, **12**(3), 361-397.

CC